GRISPE

Guidelines and **R**ecommendations for **I**ntegrating **S**pecific **P**rofiled steel sheets in the **E**urocodes (**GRISPE**)

WP3 Doc 1 Final Version 01

WP3 Background document

Working Package 3

Deliverable D 3.1

DOCUMENT CONTROL INFORMATION AND ARCHIVING

Guidelines and Recommandations for Integrating Specific Profiled Steels sheets in the Eurocodes (GRISPE)

Project co-funded under the Research Fund for Coal and Steel
Grant agreement No RFCS-CT-2013-00018
Proposal No RFS-PR-12027

Author(s)		
Palisson Anna, Sokol Palisson Consultants		
Drafting history		
Draft Version 1		*20h December 2013*
Draft Version xx		*Day Month Year*
Final Version Revision 01		*25th December 201*
Final Version Revision 02		*Day Month Year*
Final Version Revision 03		*Day Month Year*
Final Version Revision xx		*Day Month Year*
Final Version CO		*Day Month Year*
Dissemination Level		
PU	*Public*	
PP	*Restricted to the Commission Services, the Coal and Steel Technical Groups and the European Committee for Standardisation (CEN)*	
RE	*Restricted to a group specified by the Beneficiaries*	
CO	*Confidential, only for Beneficiaries (including the Commission services)*	***x***
Verification and Approval		
Coordinator David Izabel, SNPPA		
WP1 Leader SOKOL PALISSON CONSULTANTS		
Other Beneficiaries SNPPA, Bac Acier, IFL, Joris Ide, KIT, PUT		
Deliverable		
D 3.1 WP3Background document		***Due date : 30.11.2013*** ***Completion date: 25.12.2013***

1. INTRODUCTION

For architectural reasons and also in order to improve the acoustic performance perforated profiles (Fig. 1), with different types, geometries and distribution of micro-perforations on the profile web and flange, are increasingly developed and used.

Fig. 1 - Trapezoidal sheet with perforated web (Montana Bausysteme AG, Villemergen [1])

European Standard EN 1993-1-3 dealing with design rules for cold-formed members and sheeting covers only the triangular distribution of such perforations while many exist on the market.

As far as round or square holes in the flange of sheeting are concerned, they are often required for the passage of services (Fig. 2). But only plane walls without holes are covered by EN 1993-1-3.

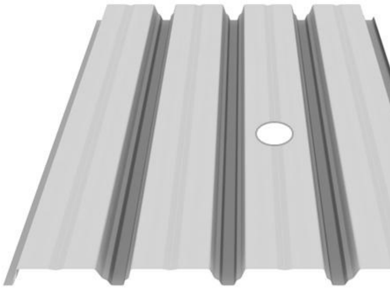

Fig. 2 - Round holes in the flange of sheeting

The aim of this document is to give a state of the art of the current European Standard EN and of the background information about steel perforated profiles and about sheeting with holes in the flange, and to emphasize the lack of data and knowledge.

2. EUROCODE

The European standard EN 1993-1-3 gives, for cold-formed members and sheeting, methods for design by calculation and for design assisted by testing. The design by calculation applies only within stated ranges of material properties and geometrical proportions for which sufficient experience and test evidence is available. These limitations do not apply to design assisted by testing.

To design steel sheeting two criteria of verification must be determined, resistance and flexion stiffness. EN 1993-1-3 provides the methodology to determine those criteria for steel sheeting only with:

- plane walls without holes
- plane walls with equilateral triangular perforation pattern (Fig. 3)

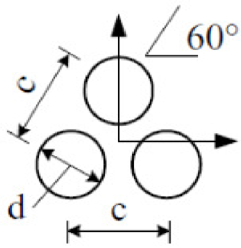

Fig. 3 - Equilateral triangular pattern

2.1. Plane without holes

The sheeting thin elements may buckle locally at a stress level lower than the yield point of steel when they are subject to compression in flexural bending and axial compression as shown in Fig. 4 [2].

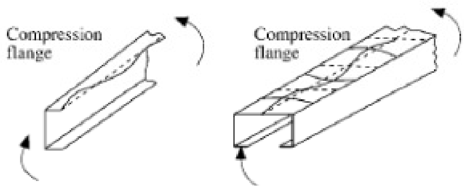

Fig. 4 - Local buckling of compression beam

An additional load can be carried by the element when the local buckling stress is reached, this phenomenon is the postbuckling strength, as shown in Fig. 5.

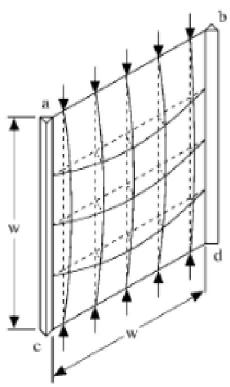

Fig. 5 - Postbuckling strength model

A nonuniform stress distribution is developed (Fig. 6)

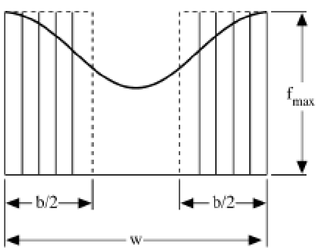

Fig. 6 - Stress distribution in stiffened compression elements

Von Karman traduced in 1910 this buckling by the following equation

$$\frac{\delta^4 w}{\delta x^4}+2\frac{\delta^4 w}{\delta x^2 \delta y^2}+\frac{\delta^4 w}{\delta y^4}=\frac{1}{D}\left(N_x\frac{\delta^2 w}{\delta x^2}+2N_{xy}\frac{\delta^2 w}{\delta x \delta y}+N_y\frac{\delta^2 w}{\delta y^2}\right)$$

$$D=\frac{Et^3}{12\left(1-\nu^2\right)}$$

The elastic local buckling stress for simply supported plate can be determined as follow:

$$f_y=\frac{\pi^2 E}{12\left(1-\nu^2\right)}*\frac{kt^2}{b_e^2}$$

This leaded Von Karman to the effective width (b_e) notion where the buckled intern part of the plate is neglected (Fig. 7)

$$\rho=\frac{b_e}{b}=\sqrt{\frac{\sigma_{cr}}{f_y}}$$

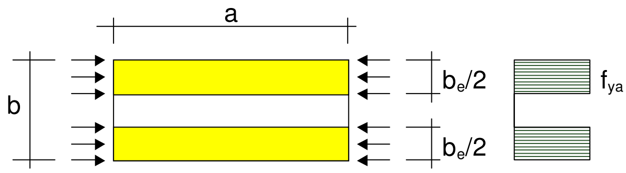

Fig. 7 - Effective width of stiffened compression elements

This theory was adapted in EN 1993-1-3 and 1993-1-5 where the effects of local and distortional buckling are taken into account in determining the resistance and stiffness of cold-formed members and sheeting. The effect of holes on the effective width is not taken into account.

2.2. Perforated sheeting

In section 10.4 of EN 1993-1-3 it is specified that perforated sheeting with the holes arranged in the shape of equilateral triangles may be designed by calculation, provided that the rules for non-perforated sheeting are modified by introducing the effective thicknesses given below.

- gross section properties may be calculated using part 5.1, but replacing t by $t_{a,eff}$ obtained from:

$$t_{a,eff} = 1{,}18\,t\left(1-\frac{d}{0{,}9a}\right)$$

where:

d	is	the diameter of the perforations;
a	is	the spacing between the centers of the perforations.

- effective section properties may be calculated using Section 5, but replacing t by $t_{b,eff}$ obtained from:

$$t_{b,eff} = t\sqrt[3]{1{,}18\left(1-d/a\right)}$$

- the resistance of a single web to local transverse forces may be calculated using part 6.1.9, but replacing t by $t_{c,eff}$ obtained from:

$$t_{c,eff} = t\left[1-(d/a)^2 s_{per}/s_w\right]^{3/2}$$

where:

s_{per}	is	the slant height of the perforated portion of the web;
s_w	is	the total slant height of the web.

The criteria of verification of a steel sheeting must take into account the effective cross-section which is impacted by holes or perforations in the web and flanges, therefore this absence in the standard EN 1993-1-3 is a real lack to correctly determine and verify the resistance of a steel sheeting. And this lack is even more disturbing and serious as several previous studies have shown that holes [3] to [8], and perforations [9] to [11] reduce the strength locally and globally and have an impact on its bending resistance [12], [13]. In the next chapter we will focus on studies performed on sheeting with holes and perforations in the webs or flanges.

3. STATE OF THE ART

3.1. Plane with holes

The review of the existing published and on-going works allowed to find several studies on steel sheeting with holes. As we will see below these studies deal on the effect of holes on local buckling and postbuckling of plates subjected to compression or shear loading.

M. Azhari [3] established a nonlinear mathematical theory for initial and post local buckling analysis of perforated thin plates based on the principle of virtual work. The results of local buckling coefficient of plates subjected to uniaxial and biaxial compressions were compared with known solutions (Fig. 8).

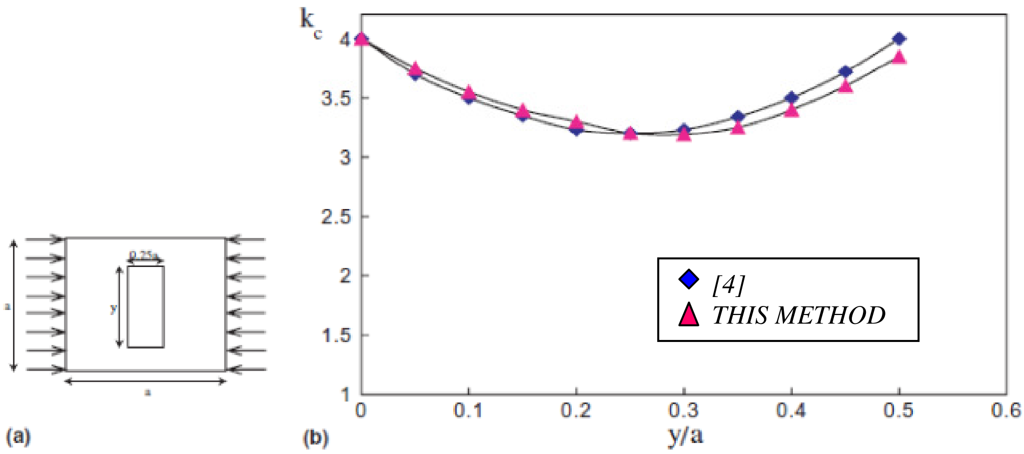

Fig. 8 - Local buckling coefficient of the perforated plate subjected to uniform compressions in one direction versus normalized rectangular hole dimension y/a.

He found that the presence of holes in structural members resulted in changes in the stress distribution within the member and consequently a reduction in the local buckling capacity of the plate. Therefore with increasing hole size parameters, strength of the perforated plate in the post local buckling phase decreased.

F-Y. Chow investigated the buckling behaviour of square plates containing holes and subjected to uniaxial or biaxial compression [5] or to in-plane shear loading [6]. He carried out parallel studies using experimental and computational methods. He found that the buckling coefficient decreased when both holes, square and circular, increased, and observed that introduction of considered types and sizes of holes rapidly reduces the strength of the plate in which the ratio width/thickness (a/t) is smaller than 50, while for higher value reduces of strength is progressive (Fig. 9).

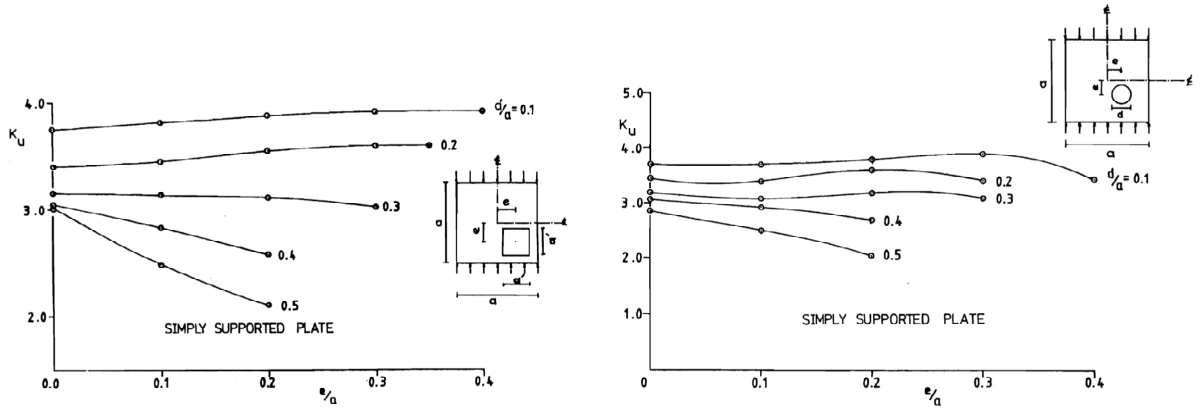

Fig. 9 Buckling coefficients for uniaxial loading for a plate with square and circular hole

The eight types of curves presented in the paper [6] can be directly used in the design process. The method can be applied for rectangular plates also.
For plates under uniform shear loading, two opposing results were obtained for holes located in the compression and tension diagonals; in the former case, the eccentricity reduced the buckling coefficient and in the latter, increased it.

J.K. Paik [7] investigated the ultimate strength characteristics of perforated steel plates under edge shear loads. He carried out a series of ANSYS elastic–plastic large deflection FEA with varying the cutout size as well as plate dimensions (aspect ratio and plate thickness). He confirmed that the cutout significantly reduced the plate ultimate strength. He found that the plate aspect ratio affected the ultimate strength of perforated plates to some extent when edge shear loads were predominant, while the plate thickness was not a sensitive parameter to the normalized ultimate shear strength when holding the cutout size constant.

Also, he found that the traditional approach of the plasticity correction with elastic buckling strength to estimate the so-called critical buckling strength may not be valid for perforated plates, specifically when the cutout size and/or the plate thickness are relatively large.

He developed, by regression analysis of FEA results, a closed-form empirical formula to predict the ultimate shear strength of perforated plate as a function of cutout size as well as plate dimensions.

He concluded that further studies were required for different types of loads or their combination loads or with different types or locations of cutout.

N.E. Shanmugam [8] studied post-buckling behaviour and ultimate load capacity of plates with holes (square and circular), with different boundary conditions and subjected to uniaxial or biaxial compression. Plates were analysed using the finite element method (FEM), and extensive studies were carried out covering parameters such as plate slenderness, opening size, boundary conditions and the nature of loading. He established a design formula to determine the ultimate load carrying capacity based on a best-fit regression analysis using the results from the finite element analyses.

The accuracy of the proposed formula was established by comparison with experimental values of ultimate capacity and similar finite element values. Ultimate load values are also presented in the form of charts for various values of plate slenderness and opening size. The ultimate load carrying capacity of perforated plates was found to be affected by various parameters studied. The increase in hole size and slenderness ratio resulted in a significant loss in the ultimate strength of perforated plates. The strength of perforated plates with simply supported edges was lower as compared to that of plates with clamped edges. The plates with circular holes generally had higher ultimate loads compared to the square perforated plates.

<u>The reviewer notes:</u>
The whole studies above investigated local buckling and postbuckling of plates subjected to axial compression and shear loading. There is no existing study which establishes for sheeting with holes:

- moment resistance under flexion
- web crippling resistance
- effect of combined action of support reaction and negative moment

3.2. Perforated sheeting

Several studies on sheets with triangular pattern perforations were performed.

S. C. Baik [9] proposed the following yield criterion in terms of apparent stresses of sheets with a uniform triangular pattern of round holes under biaxial loading and confirmed it by finite element analysis results (Fig. 10).

$$f_s^2 \sigma_s^{*2} + \sigma_n^{*2} - f_s \sigma_s^* \sigma_n^* + 3\sigma_{sn}^{*2} = \sigma_b^{*2}.$$

Further incorporating this yield stress he obtained a yield function containing anisotropic coefficients.

$$7.56\,|\sigma_{xy}^*|^{2.1} + 1.36\,|\sigma_x^*|^{2.1} + 1.39\,|\sigma_y^*|^{2.1} + |\sigma_x^* - \sigma_y^*|^{2.1} = (0.31\,\sigma_b)^{2.1}.$$

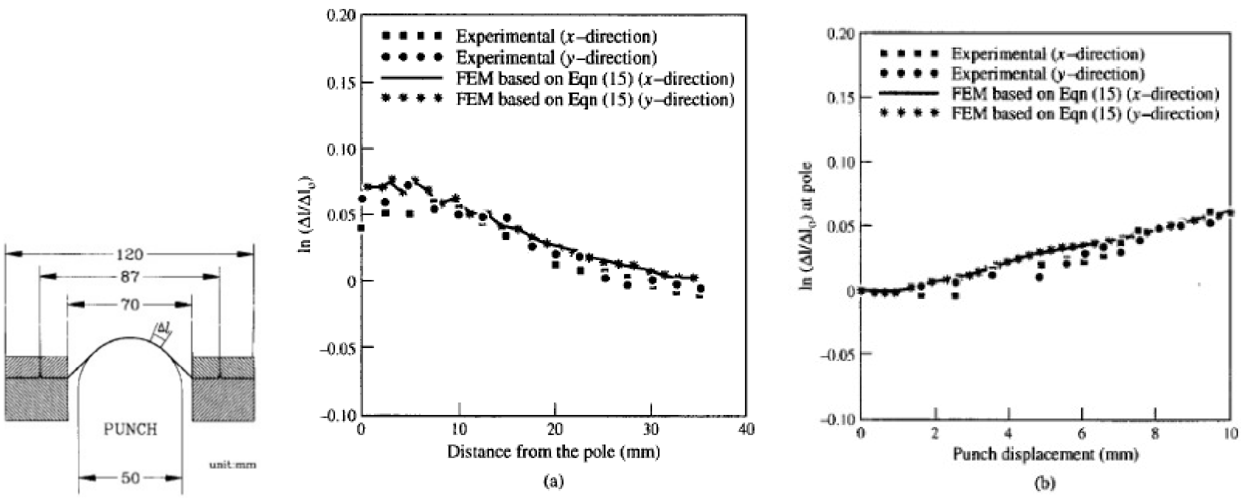

Fig. 10 - (a) Plots of measured and calculated linear strains along the surface of the sheet in the x and y directions at a dome height of 9.3 mm; and (b) the measured and calculated strains at the pole as a function of punch displacement in the x and y directions.

Y-C. Lee [10] investigated the plastic behavior of perforated sheets with low ligament ratios (Fig. 11) , he proposed a yield criterion for the perforated sheets in terms of apparent stresses by employing the equivalent-continuum approach.

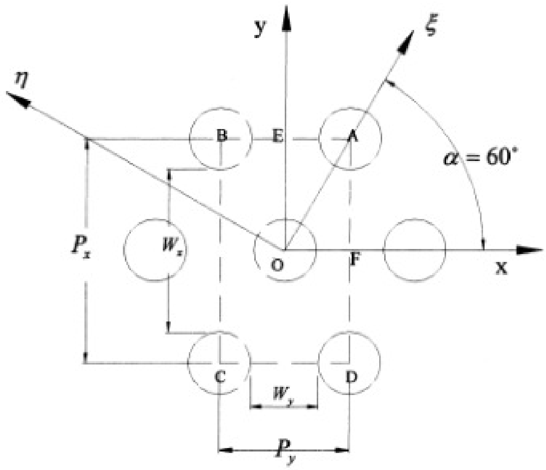

Fig. 11 - Round holes arranged in a triangular pattern.

Obtained yield criteria:

- For yielding along AB

$$\left(\frac{f}{\rho_x}\right)^2 S_x^2 - \left(\frac{f}{\rho_x\rho_y}\right) S_x S_y + \left(\frac{1}{\rho_y^2}\right) S_y^2 = Y_b^2.$$

- For yielding along AO:

$$\frac{1}{16}\left[\left(\frac{f}{\rho_x}\right)^2 - \frac{3f}{\rho_x\rho_y} + \frac{9}{\rho_y^2} + \frac{9}{\rho_y^2}\right] S_x^2 + \frac{1}{16}\left[6\left(\frac{f}{\rho_x}\right)^2 - \frac{10f}{\rho_x\rho_y} + \frac{6}{\rho_y^2} - \frac{18}{\rho_y^2}\right] S_x S_y + \frac{1}{16}\left[9\left(\frac{f}{\rho_x}\right)^2 - \frac{3f}{\rho_x\rho_y} + \frac{1}{\rho_y^2} + \frac{9}{\rho_y^2}\right] S_y^2 = Y_b^2.$$

The effectiveness of the proposed yield criterion was then demonstrated by comparing the predicted values of apparent yield stresses and apparent strain ratios with results obtained from finite-element analysis and experiment (Fig.12).

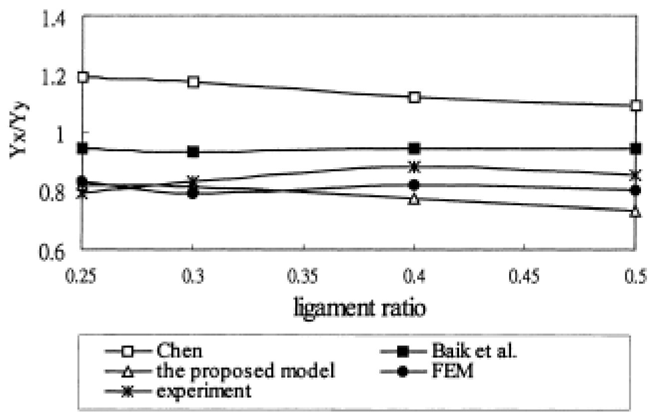

Fig. 12 - Comparison of the apparent yield stress ratio (Yx/Yy).

V. V. Degtyarev [11] studied critical elastic buckling load of uniformly uniaxial compressed isotropic plates perforated in equilateral triangular patterns using FEM (Fig. 13).

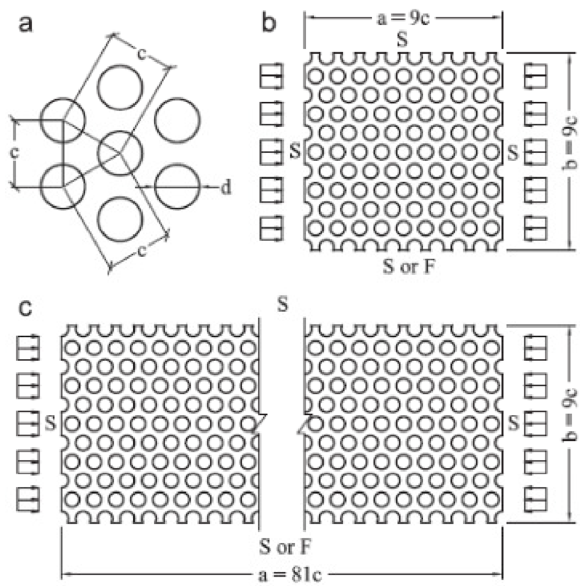

Fig. 13 -Studiedperforatedplates.(a)Equilateraltriangularperforationpattern;
(b)Squareplates;and(c)Rectangularplates.S¼simplysupportedside;F¼freeside

The effect of perforations on the critical elastic buckling load was determined. His main conclusions were:

- Critical elastic buckling load of perforated plates decreased as the hole diameter-to-spacing ratio, d/c, increased (Fig. 14)

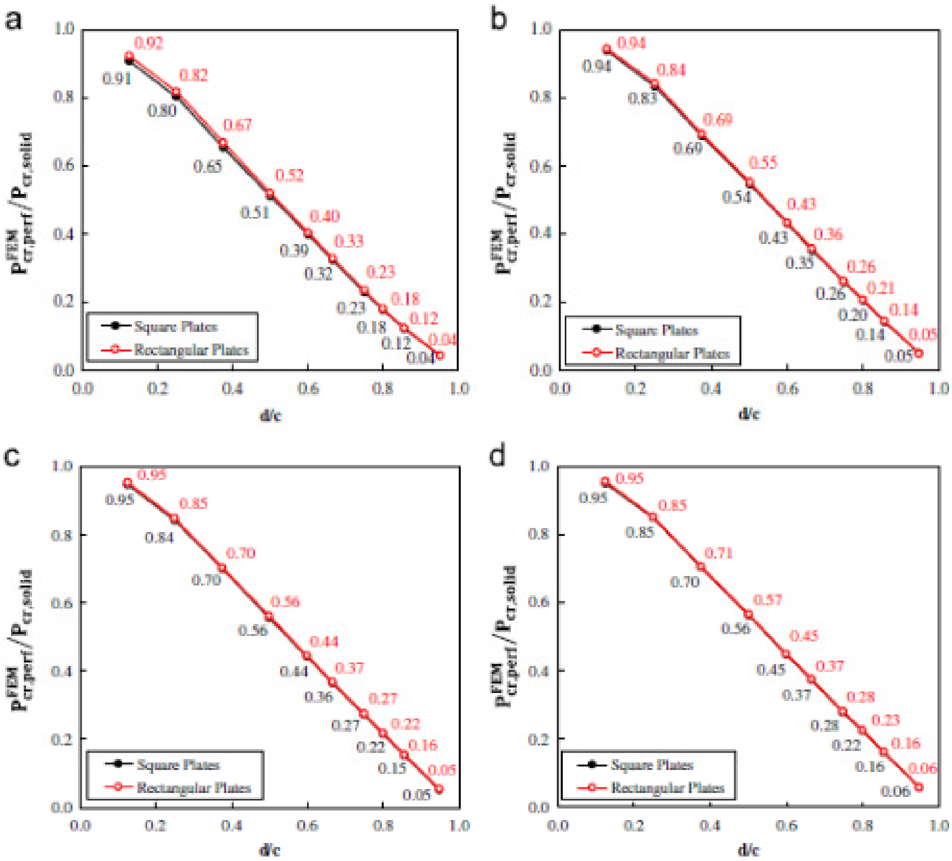

Fig. 14 - Effect of hole diameter-to-spacing ratio on critical elastic buckling load of perforated stiffened elements.(a) t¼b/20; (b) t¼b/40; (c) t¼b/60; and(d) t¼b/80.

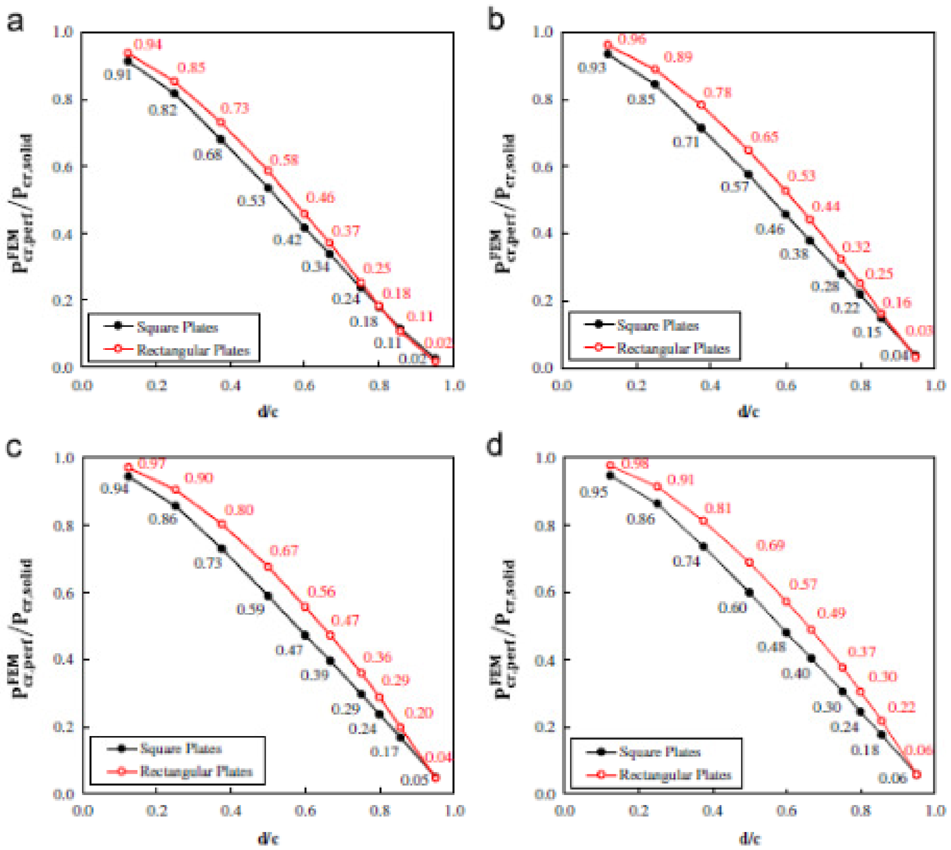

Fig.15 - Effect of hole diameter-to-spacing ratio on critical elastic buckling load of perforated unstiffened elements.(a) t¼b/20; (b) t¼b/40; (c) t¼b/60; and(d) t¼b/80.

- Stiffened square and rectangular elements demonstrated approximately the same critical elastic buckling load reduction for each considered d/c ratio.
- Unstiffened square elements demonstrated up to 30% greater critical elastic buckling load reduction due to the perforations when compared to unstiffened rectangular elements.
- For the most d/c values, the difference in the critical elastic buckling load reduction of the stiffened and unstiffened square elements was within 9%, but it achieved 88% for d/c=0.95 and b/t=20 (Fig. 14 and Fig. 15).
- A series of design formulas for predicting critical elastic buckling stress based on reduction coefficient approach and equivalent thickness approach was developed using multiple nonlinear regression analysis of the FEM results. In the equivalent thickness approach, the critical elastic buckling stress of perforated plates is calculated as follows:

  $$f_{cr} = k\frac{\pi^2 E}{12(1-\nu^2)}\left(\frac{t_{eq}}{b}\right)^2,$$

  the equivalent thickness is determined as follows

  $$t_{eq} = \sqrt{k_p}t,$$

  The author noted that when critical elastic buckling is calculated not in term of stress but in terms of distributed or total loads w_{cr} and P_{cr} , the equivalent thickness shall be determined using the following t_{eq}.

$$w_{cr} = k\frac{\pi^2 E}{12(1-\nu^2)}\frac{t_{eq}^3}{b^2},$$

$$P_{cr} = k\frac{\pi^2 E}{12(1-\nu^2)}\frac{t_{eq}^3}{b},$$

$$t_{eq} = \sqrt[3]{k_p}t,$$

<u>The reviewer notes:</u>
These three studies above deal with plates perforated in triangular patterns and don't provide information about quadratic patterns.

Studies about different arrays of holes were performed in Germany by Th. Misiek [12], [13], and K. Kathage [14]. The latter carried out a numerical analysis of perforated trapezoidal sheeting with quadratic arrays of the holes. He determined effective stiffness and deformation behaviour. The buckling coefficients for perforated plates under uniform uniaxial compression-loading and for infinitely long perforated plates under shear loading were derived as a base for the calculation of the effective width of a cross-section.

Th. Misiek [12] investigated the structural behavior of perforated thin-walled components with different hole patterns (Fig. 16) and developed on this basis a calculation method to determine the bearing capacity of fully or partially perforated thin-walled components such as trapezoidal or corrugated profiles.

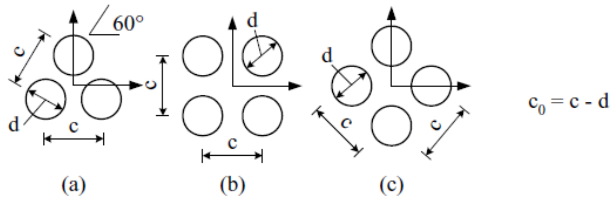

Fig. 16 - Perforation patterns

He normalized effective stiffness as a function of t/c for different perforation patterns, then he determined buckling stress and effective buckling stress which leaded to effective width and to bending moment, shear resistance and web crippling.

Here is a comparison of T. Misiek study, on the right column, with the Eurocode 3 rules on the left column

<u>Plane Elements with intermediate stiffeners EC3-1-3: 5.5.3.3 (4)</u>

<table>
<tr><td colspan="2">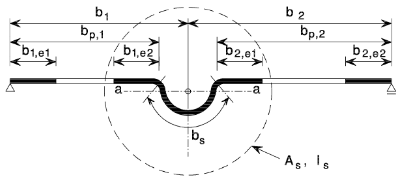
</td></tr>
<tr><th>EUROCODE RULES</th><th>T. MISIEK STUDY</th></tr>
<tr><td>Plate slenderness $\bar{\lambda}_p$ according to EN 1993-1-5

Plane Elements (part 4.4)</td><td>$\bar{\lambda}_{p,p} = \sqrt{\frac{\frac{c_0}{c} \cdot f_y}{\sigma_{ki,p}}}$</td></tr>
</table>

$$\bar{\lambda}_p = \sqrt{\frac{f_y}{\sigma_{cr}}} = \frac{\bar{b}/t}{28{,}4\ \varepsilon\ \sqrt{k_\sigma}}$$

$\bar{b} = b_p$

$$\varepsilon = \sqrt{\frac{235}{f_y\ \ [\text{N/mm}^2]}}\ .$$

internal compression elements:

$\rho = 1{,}0$ for $\bar{\lambda}_p \leq 0{,}673$

$\rho = \dfrac{\bar{\lambda}_p - 0{,}055\,(3+\psi)}{\bar{\lambda}_p^2} \leq 1{,}0$ for $\bar{\lambda}_p > 0{,}673$, where $(3+\psi) \geq 0$

$$\sigma_{ki,p} = \sigma_{cr,p} = k_\sigma\,(\psi) \cdot k_{11} \cdot \sigma_E$$

$$k_\sigma(\psi = 1) = \left(\frac{m^2}{\bar{\alpha}^2} + q \cdot \frac{\bar{\alpha}^2}{m^2}\right) + p \cdot \varsigma = 2 + 2 \cdot \varsigma$$

$$\varsigma = \frac{K_{12} + 2 \cdot K_{44}}{\sqrt{K_{11} \cdot K_{22}}}\ .$$

(EC3-1-5:A1):

$$\sigma_E = \frac{\pi^2\ E\ t^2}{12\left(1-\nu^2\right)b^2}$$

$$\rho = \frac{b_{eff}}{b} = \frac{c_0}{c} \cdot \left(\frac{1}{\bar{\lambda}_{p,p}} - \frac{0{,}22}{\bar{\lambda}_{p,p}^2}\right) \leq \frac{c_0}{c}\ .$$

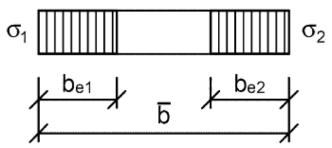

$\psi = 1$: $\quad b_{eff} = \rho\ \bar{b}$

$b_{e1} = 0{,}5\ b_{eff}$ $\quad$ $b_{e2} = 0{,}5\ b_{eff}$

Flange with intermediate stiffener (5.5.3.4.2)

(2) For one central flange stiffener, the elastic critical buckling stress $\sigma_{cr,s}$ should be obtained from:

$$\sigma_{cr,s} = \frac{4{,}2\,k_w\,E}{A_s}\sqrt{\frac{I_s\ \ t^3}{4\ b_p^2\ \left(\ 2\ b_p\ +\ 3\ b_s\ \right)}}$$

with

$$A_s = t\,(b_{1,e2} + b_{2,e1} + b_s)$$

(3) For two symmetrically placed flange stiffeners, the elastic critical buckling stress $\sigma_{cr,s}$ should be obtained from:

$$\sigma_{cr,s} = \frac{4{,}2\ k_w\ E}{A_s}\sqrt{\frac{I_s\ \ t^3}{8\ b_1^2\ \left(\ 3\ b_e\ -\ 4\ b_1\ \right)}}$$

with:

$$b_e = 2b_{p,1} + b_{p,2} + 2b_s$$

$$b_1 = b_{p,1} + 0{,}5\,b_r$$

with

$$A_s = t\,(b_{1,e2} + b_{2,e1} + b_s)$$

$$\sigma_{cr,s,p} = \sqrt{k_{11} \cdot d_{11}} \cdot \sigma_{cr,s}$$

with

$$A_s = A_{s,p}$$

K_w is a coefficient that allows for partial rotational restraint of the stiffened flange by the webs or other adjacent elements, see (5) and (6). For the calculation of the effective cross-section in axial compression the value kw = 1,0 (5) - if $l_b/s_w \geq 2$: $k_w = k_{wo}$ - if $l_b/s_w < 2$: $k_w = k_{wo} - (k_{wo} - 1)\left[\frac{2l_b}{s_w} - \left(\frac{l_b}{s_w}\right)^2\right]$	$k_w = \begin{cases} k_{w0} + (k_{w0} - 1)\cdot\left(\left(\frac{l_{b,p}}{s_w}\right)^2 - 2\cdot\frac{l_{b,p}}{s_w}\right) & \text{für } \frac{l_b}{s_w} < 2 \\ k_{w0} & \frac{l_b}{s_w} \geq 2 \end{cases}$
for a compression flange with one intermediate stiffener: $l_b = 3{,}07\sqrt[4]{\frac{I_s\, b_p^2\,(2\,b_p + 3\,b_s)}{t^3}}$ $k_{wo} = \sqrt{\frac{s_w + 2\,b_d}{s_w + 0{,}5\,b_d}}$	$k_{w0} = \sqrt{\frac{\frac{k_{11,1}}{k_{11,2}}\cdot s_w + 2\cdot b_1}{\frac{k_{11,1}}{k_{11,2}}\cdot s_w + 0{,}5\cdot b_1}}$ $l_b = 3{,}65\cdot\sqrt[4]{I_r\cdot b_p^3\cdot\frac{1+3\cdot s_r/b_p}{k_{11,1}\cdot t^3}} = 3{,}65\cdot\sqrt[4]{\frac{d_{11}}{k_{11,1}}\cdot I_r\cdot b_p^3\cdot\frac{1+3\cdot s_r/b_p}{t^3}}$ with $s_r = 0{,}5 * b_s$ $b_1 = b_0$
for a compression flange with two intermediate stiffeners: $l_b = 3{,}65\sqrt[4]{I_s\, b_1^2\,(3\,b_e - 4\,b_1)/t^3}$ $k_{wo} = \sqrt{\frac{(2\,b_e + s_w)(3\,b_e - 4\,b_1)}{b_1\,(4\,b_e - 6\,b_1) + s_w\,(3\,b_e - 4\,b_1)}}$	$k_{w0} = \sqrt{\frac{\left(2\cdot b_1 + \frac{k_{11,1}}{k_{11,2}}\cdot s_w\right)\cdot(3\cdot b_1 - 4\cdot b_k)}{b_k\cdot(4 - b_1 - 6\cdot b_k) + \frac{k_{11,1}}{k_{11,2}}\cdot s_w\cdot(3\cdot b_1 - 4\cdot b_k)}}$ $l_b = 3{,}65\cdot\sqrt[4]{I_{r,p}\cdot b_p^3\cdot\frac{3\cdot b_1/b_k - 4}{k_{11,1}\cdot t^3}} = 3{,}65\cdot\sqrt[4]{\frac{d_{11}}{k_{11,1}}\cdot I_r\cdot b_p^3\cdot\frac{3\cdot b_1/b_k - 4}{t^3}}$ with $b_k = b_p + b_r/2$ $b_1 = b_0$ 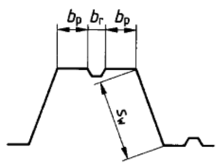

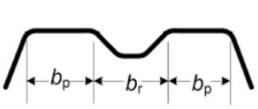

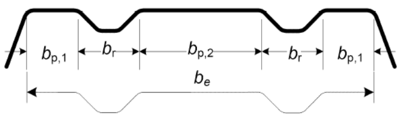

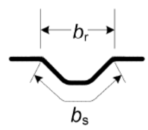

Reduction factor χ_d 5.5.3.1 (7):

$$\chi_d = 1{,}0 \qquad \text{if } \bar{\lambda}_d \leq 0{,}65$$

$$\chi_d = 1{,}47 - 0{,}723\bar{\lambda}_d \qquad \text{if } 0{,}65 < \bar{\lambda}_d < 1{,}38$$

$$\chi_d = \frac{0{,}66}{\bar{\lambda}_d} \qquad \text{if } \bar{\lambda}_d \geq 1{,}38$$

$\bar{\lambda}_d = \sqrt{f_{yb}/\sigma_{cr,s}}$	$\bar{\lambda}_d = \sqrt{f_{yb}/\sigma_{cr,s,p}}$

Webs with up to tow intermediate stiffeners (5.5.3.4.3)

EC3-1-3:5.5.3.4.3 (5):

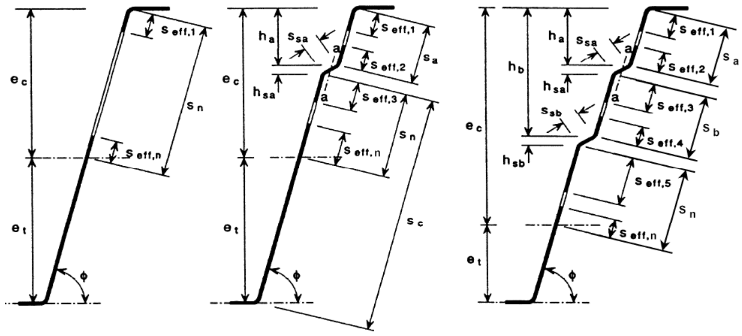

(5) $s_{eff,0} = 0,76\,t\,\sqrt{E/(\gamma_{M0}\,\sigma_{com,Ed})}$ $s_{eff,1} = s_{eff,0}$ $s_{eff,2} = (1 + 0,5h_a/e_c)\,s_{eff,0}$ $s_{eff,3} = [1 + 0,5(h_a + h_{sa})/e_c]\,s_{eff,0}$ $s_{eff,4} = (1 + 0,5h_b/e_c)\,s_{eff,0}$ $s_{eff,5} = [1 + 0,5(h_b + h_{sb})/e_c]\,s_{eff,0}$ $s_{eff,n} = 1,5s_{eff,0}$ → EC3-1-3:5.5.3.4.3 (6)	$s_{ef1,p} = 0,54\cdot t\cdot\sqrt{\frac{k_{11}\cdot E}{\sigma_1}\cdot(\varsigma+1)}$ $s_{efn,p} = \left(1{,}18\cdot\sqrt{\frac{4\cdot\varsigma+5}{\varsigma+1}}-1\right)\cdot s_{ef1,p}$ $s_{efi,tp} = s_{efn,tp} + (s_{ef1,tp} - s_{efn,tp})\cdot\frac{\sigma_i}{\sigma_1}$ $\varsigma = \frac{k_{44}+0{,}3\cdot(k_{12}-k_{44})}{k_{11}}$ triangular holes ζ = 1,0
(7) For a single stiffener, or for the stiffener closer to the compression flange in webs with two stiffeners, the elastic critical buckling stress $\sigma_{cr,sa}$ should be determined using: $\sigma_{cr,sa} = \frac{1{,}05\,k_f\,E\sqrt{I_s\,t^3\,s_1}}{A_{sa}\,s_2\,(s_1 - s_2)}$ with $s_2 = s_1 - s_a - 0,5\,s_{sa}$ for a singel stiffener $s_1 = 0,9\,(s_a + s_{sa} + s_c)$ For the stiffener closer to the comression flange, in webs with two stiffeners $s_1 = s_a + s_{sa} + s_b + 0,5(s_{sb} + s_c)$	$\sigma_{cr,sa,p} = \sqrt{k_{11}\cdot d_{11}}\cdot\sigma_{cr,sa}$ with $A_{sa} = A_{sa,p}$ and $A_{sb} = A_{sb,p}$

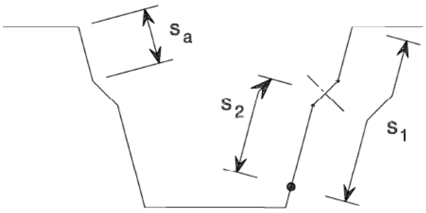

The effective area shoul be obtained from the following:

For a single stiffener, or for the stiffener closer to the compression flange

$$A_{sa} = t\,(s_{eff,2} + s_{eff,3} + s_{sa})$$

For a second stiffener

$$A_{sb} = t\,(s_{eff,4} + s_{eff,5} + s_{sb})$$

(9) For a single stiffener, or for the stiffener closer to the compression flange in webs with two stiffeners, the reduced effective area $A_{sa,red}$ should be determinded from:

$$A_{sa,red} = \frac{\chi_d \, A_{sa}}{1-(h_a + 0{,}5 h_{sa})/e_c} \quad \text{but } A_{sa,red} \le A_{sa}$$

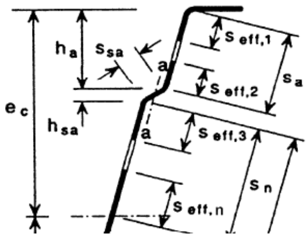

Sheeting with flange stiffeners and web stiffeners: (5.5.3.4.4)

(1) Interaction between the distortional buckling (flexural buckling of the flange stiffeners and the web stiffeners) should be obtained from

$$\sigma_{cr,mod} = \frac{\sigma_{cr,s}}{\sqrt[4]{1+\left[\beta_s \dfrac{\sigma_{cr,s}}{\sigma_{cr,sa}}\right]^4}}$$

with

β_s = 1 - $(h_a + 0{,}5\, h_{ha}) / e_c$ for a profile in bending;

β_s = 1 for a profile in axial compression.

$$N_{el,p} = \left(\frac{1}{N_{rel,p}^4} + \frac{\delta^4}{N_{sel,p}^4}\right)^{-\frac{1}{4}}$$

with

$$\delta = \frac{\sigma(h'_a)}{\sigma_1} \cdot \frac{A_{s,p}}{A_{r,p}}$$

$$\frac{N_{rel,p}}{A_{r,p}} = \sigma_{cr,s,p}$$

$$\frac{N_{sel,p}}{A_{s,p}} = \sigma_{cr,sa,p}$$

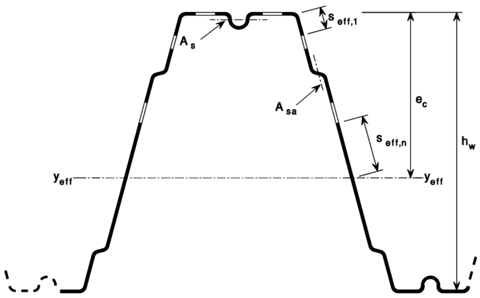

Figure 5.16: Trapezoidal profiled sheeting with flange stiffeners and web stiffeners

Bending Moment (6.1.4)

$M_{c,Rd} = W_{eff} f_{yb} / \gamma_{M0}$	Fully perforated trapezoidal sheeting $M_{R,k} = W_{ef} \cdot \frac{c_0}{c} \cdot f_y$
	Flanges without perforation and partially perforated webs: Moment resistance of the unperforated flange $M_{R,k} = \frac{I_{ef}}{z_{max}} \cdot f_y$ Moment resistance of the web $M_{R,k} = \frac{I_{ef}}{z_{tp}} \cdot \frac{1}{d_{11}} \cdot \frac{c_0}{c} \cdot f_y$ with z_{tp}: maximum ordinate of the transition from the unperforated to the perforated section and $\frac{1}{d_{11}} \cdot \frac{c_0}{c} \leq 1$
	Flanges fully perforated and partially perforated webs: Moment resistance of the fully perforated flange $M_{R,k} = \frac{I_{ef}}{z_{max}} \cdot \frac{1}{d_{11}} \cdot \frac{c_0}{c} \cdot f_y$ Moment resistance of the web $z \geq z_{tp}$ $M_{R,k} = \frac{I_{ef}}{z_{tp}} \cdot \frac{1}{d_{11}} \cdot \frac{c_0}{c} \cdot f_y$ or $M_{R,k} = \frac{I_{ef}}{z_{tp}} \cdot f_y$ with $\frac{1}{d_{11}} \cdot \frac{c_0}{c} \leq 1$

Shear Force (6.1.5)

(1) Shear resistance $V_{b,Rd} = \frac{\frac{h_w}{\sin\phi} t f_{bv}}{\gamma_{M0}}$ Webs without longitudinal stiffeners $\bar{\lambda}_w = 0{,}346 \frac{s_w}{t} \sqrt{\frac{f_{yb}}{E}}$ Webs with longitudinal stiffeners	Shear resistance $V_{d,p} = \frac{c_0}{c} \cdot \tau_d \cdot s_w \cdot t \cdot \sin\varphi$ Webs without longitudinal stiffeners $\lambda_{w,p} = \frac{s_w}{t} \cdot \frac{2{,}31}{\sqrt{k_{\tau,p}}} \cdot \sqrt{\frac{\frac{c_0}{c} \cdot f_y}{E}}$ with

$$\bar{\lambda}_w = 0{,}346\,\frac{s_d}{t}\sqrt{\frac{5{,}34\,f_{yb}}{\kappa_\tau\;E}} \geq 0{,}346\,\frac{s_p}{t}\sqrt{\frac{f_{yb}}{E}}$$

with

$$k_\tau = 5{,}34 + \frac{2{,}10}{t}\left(\frac{\Sigma I_s}{s_d}\right)^{1/3}$$

Relative web slenderness	Web without stiffening at the support	Web with stiffening at the support [1]
$\bar{\lambda}_w \leq 0{,}83$	$0{,}58\,f_{yb}$	$0{,}58\,f_{yb}$
$0{,}83 < \bar{\lambda}_w < 1{,}40$	$0{,}48 f_{yb}/\bar{\lambda}_w$	$0{,}48 f_{yb}/\bar{\lambda}_w$
$\bar{\lambda}_w \geq 1{,}40$	$0{,}67 f_{yb}/\bar{\lambda}_w^2$	$0{,}48 f_{yb}/\bar{\lambda}_w$

[1] Stiffening at the support, such as cleats, arranged to prevent distortion of the web and designed to resist the support reaction.

$$k_{\tau,p} = \begin{cases} k_{11}\cdot\left(3{,}293 + 2{,}286\cdot\varsigma - 0{,}24\cdot\varsigma^2\right) & \text{für } \varsigma \leq 1 \\ k_{11}\cdot\sqrt{\varsigma}\cdot\left(4{,}757 + \dfrac{0{,}874}{\varsigma^2} - \dfrac{0{,}283}{\varsigma^4}\right) & \text{für } \varsigma > 1 \end{cases}$$

Webs with longitudional stiffeners

$$\bar{\lambda}_w = 2{,}31\,\frac{s_1}{t}\sqrt{\frac{\frac{c_0}{c}}{\kappa_{\tau,p}}\,\frac{f_y}{E}}$$

with

$$k_{\tau,p} = \begin{cases} k_{11}\cdot\left(3{,}293 + 2{,}286\cdot\varsigma - 0{,}24\cdot\varsigma^2\right) + \dfrac{2{,}1}{t}\cdot\sqrt[3]{k_{11}^2\cdot d_{11}\cdot\dfrac{I_s}{s_1}} & \varsigma \leq 1 \\ k_{11}\cdot\sqrt{\varsigma}\cdot\left(4{,}757 + \dfrac{0{,}874}{\varsigma^2} - \dfrac{0{,}283}{\varsigma^4}\right) + \dfrac{2{,}1}{t}\cdot\sqrt[3]{k_{11}^2\cdot d_{11}\cdot\dfrac{I_s}{s_1}} & \varsigma > 1 \end{cases} \quad \text{für}$$

and

$$\bar{\lambda}_w \geq 2{,}31\,\frac{s_m}{t}\sqrt{\frac{\frac{c_0}{c}}{\kappa_{\tau,p}}\,\frac{f_{yb}}{E}}$$

with

$$k_{\tau,p} = \begin{cases} k_{11}\cdot\left(3{,}293 + 2{,}286\cdot\varsigma - 0{,}24\cdot\varsigma^2\right) & \text{für } \varsigma \leq 1 \\ k_{11}\cdot\sqrt{\varsigma}\cdot\left(4{,}757 + \dfrac{0{,}874}{\varsigma^2} - \dfrac{0{,}283}{\varsigma^4}\right) & \text{für } \varsigma > 1 \end{cases}$$

	τ_d/β_S für Stege ohne Stützbleche über den Auflagern	τ_d/β_S für Stege mit Stützblechen über den Auflagern
$\lambda_w \leq 2{,}1$	0,67	0,67
$2{,}1 < \lambda_w \leq 4{,}0$	$1{,}4/\lambda_w$	$1{,}4/\lambda_w$
$4{,}0 < \lambda_w$	$5{,}6/\lambda_w^2$	$1{,}4/\lambda_w$

Based on comprehensive numerical and experimental investigations on web crippling (Fig. 17), it

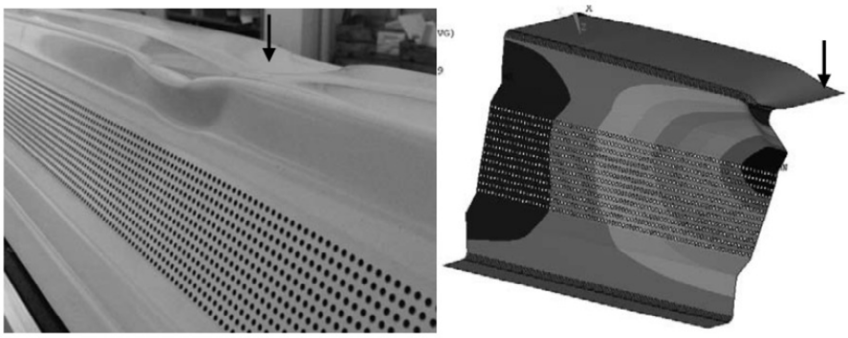

Fig. 17 - Web crippling failure at supports

could be shown for fully and partially perforated trapezoidal profiles, that the influence of the perforation can be expressed with the application according to DIN 18807-1 [15] and DIN 18807-6 [16] of a factor Cp for fully perforated webs.

$$R_{w,Rd,p} = C_p \cdot R_{w,Rd}$$

$$C_p = \sqrt{\frac{c_0}{c}\cdot\frac{k_{\sigma,p}}{4}} = \sqrt{\frac{c_0}{c}\cdot\frac{k_{11} + k_{44} + 0.3\cdot\left(k_{12} - k_{44}\right)}{2}}$$

And C_{tp} for partially perforated webs to the capacities of the unperforated sheeting according to EN 1993-1-3 and EN 1999-1-4.

$$R_{w,Rd,tp} = C_{tp} \cdot R_{w,Rd}$$

$$C_{tp} = \begin{cases} 1.0 & b_1 > \beta_{tp} \cdot b \\ \dfrac{\beta_1}{\beta_{tp}} \cdot \dfrac{s_w}{b_B} + C_{tp}^* \cdot \left(1 - \dfrac{\beta_1}{\beta_{tp}} \cdot \dfrac{s_w}{b_B}\right) & \text{for } r \cdot \tan\dfrac{\phi}{2} < b_1 \le \beta_{tp} \cdot b_B \\ C_p & b_1 \le r \cdot \tan\dfrac{\phi}{2} \end{cases}$$

with

$$C_{tp}^* = 0.59 + 0.41 \cdot \sqrt{\frac{c_0}{c} \cdot \frac{k_{\sigma,p}}{4}}$$

and

$$\beta_{tp} = 2.57 \cdot \left(0.70 - 0.09 \cdot \sqrt{\frac{r}{t}}\right) \cdot \left(0.57 - 0.37 \cdot \left(\frac{\phi}{90}\right)^2\right)$$

For stiffened webs:

$$R_{w,Rd} = \kappa_s \cdot R_{w,Rd}$$

with

$$\kappa_s = 1{,}0$$

For design purpose, to take into account the scatter of results, the characteristic values should be used with the following equations.

$$C_{tp,k}^* = 0.92 \cdot C_{tp}^*$$

$$\beta_{tp,k} = \beta_{tp} \cdot \frac{1 - C_{tp,k}^*}{1 - C_{tp}^*}$$

A calculation procedure for these factors was described (Fig. 18).

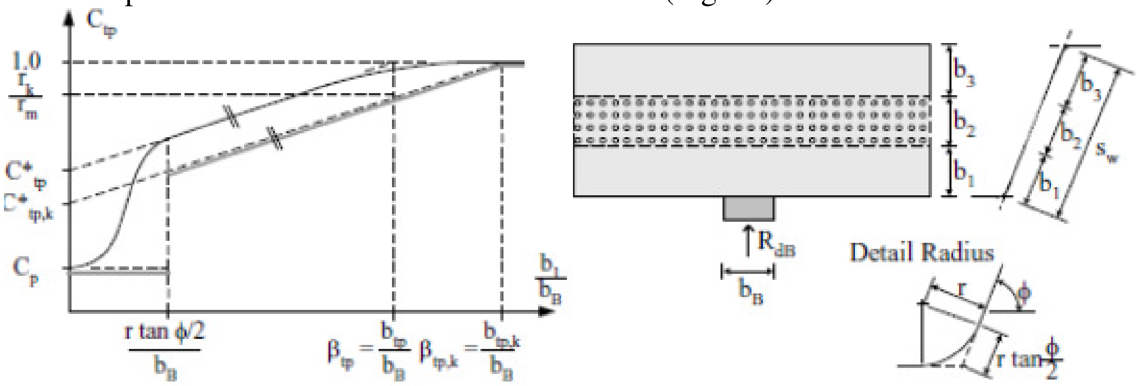

Fig. 18 - C_{tp} in dependence of b1 to b_B and the corresponding dimensions of the sheeting

Numerical investigations with the finite-elements method allow the verification of these theoretically derived calculation procedures. And all theoretical considerations or numerical studies results could be verified by comparison with experimental results from a extensive database as well as specially conducted for this work attempts (Fig. 19).

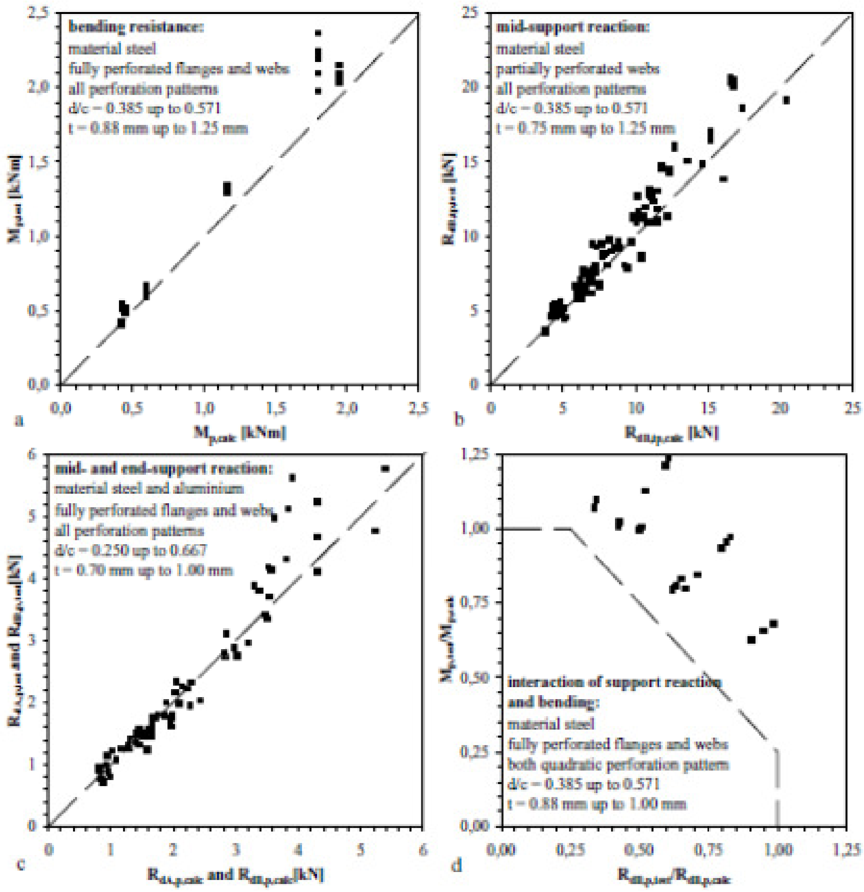

Fig. 19 - Comparison of calculated load-bearing capacities with test results

4. CONCLUSIONS

As we could see in this state of the art the European Standard EN 1993-1-3 dealing with design rules for cold-formed members and sheeting only covers plane walls without holes and plane walls with equilateral triangular perforation pattern. The background information about sheeting with holes only deals with buckling and postbuckling of plates with holes subjected to compression and shear loadings, and doesn't give any data about moment resistance, web crippling resistance and interaction moment-reaction resistance. As far as are perforated sheeting with triangular and quadratic pattern perforations are concerned, some useful information found in the literature was given by Th. Misiek investigations on the effective width and web crippling resistance. However, this investigation was based on numerical computer analysis that doesn't lead directly to the analytical formulation.

Therefore a series of tests and analytical investigations should be performed in order to acquire data on resistance and stiffness of the steel decks with holes and in order to confirm and complete design rules determined by the unique investigation about triangular and quadratic pattern perforations, existing in the background.

REFERENCES

[1] TH. MISIEK, H. SAAL, K. KATHAGE "TRAGFAHIGKEIT PERFORIERTER DUNNWANDIGER BAUTEILE" STAHLBAU 78, 2009

[2] YU, W.W. “COLD-FORMED STEEL STRUCTURES” *STRUCTURAL ENGINEERING HANDBOOK,* ED. CHEN WAI-FAH BOCA RATON: CRC PRESS LLC, 1999
[3] M. AZHARI, A. R. SHAHIDI, M. M. SAADATPOUR "LOCAL AND POST LOCAL BUCKLING OF STEPPED AND PERFORATED THIN PLATES" 2005
[4] C.J. BROWN, A.L. YETTRAM, M. BURNETT, STABILITY OF PLATES WITH RECTANGULAR HOLES, J. STRUCT. ENG. 1131111–1116, 1987
[5] F-Y. CHOW, R. NARAYANAN "BUCKLING OF PLATES CONTAINING OPENINGS" 1984
[6] R. NARAYANAN, F-Y. CHOW "STRENGTH OF BIAXIALLY COMPRESSED PERFORATED PLATES" 1984
[7] PAIK J.K. "ULTIMATE STRENGTH OF PERFORATED STEEL PLATES UNDER EDGE SHEAR LOADING", THIN-WALLED STRUCTURES 45, 2007
[8] SHANMUGAM N.E "DESIGN FORMULA FOR AXIALLY COMPRESSED ERFORATED PLATES" THIN-WALLED STRUCTURES 34, 1999
[9] SEUNG CHUL BAIK*, HEUNG NAM HAN*, SANG HEON LEE*, KYU HWAN OH * and DONG NYUNG LEE, "PLASTIC BEHAVIOUR OF PERFORATED SHEETS UNDER BIAXIAL STRESS STATE", LNT. J. MECH. SCI. VOL. 39, NO. 7, PP. 781- 793. 1997
[10] Y-C LEE, F-K. CHEN; "YIELD CRITERION FOR A PERFORATED SHEET WITH A UNIFORM TRIANGULAR PATTERN OF ROUND HOLES AND A LOW LIGAMENT RATIO", DEPARTMENT OF MECHANICAL ENGINEERING, NATIONAL TAIWAN UNIVERSITY, 1 ROOSEVELT ROAD, SECT. 4, TAIPEI 10764, TAIWAN, ROC, RECEIVED 28 FEBRUARY 1999
[11] V.V DEGTYAREV, N.V DEGTYAREVA "ELASTIC STABILITY OF UNIFORMLY COMPRESSED PLATES PERFORATED IN TRIANGULAR PATTERNS", THIN-WALLED STRUCTURES 52 (2012) 165–173
[12] T.MISIEK, 2008, TRAGVERHALTEN DÜNNWANDIGER BAUTEILE AUS PERFORIERTEN BLECHEN (DESCRIBED BY ZBP) PHD IN GERMAN, UNIVERSITÄT FRIDERICIANA ZU KARLSRUHE, 2008
[13] T.MISIEK, H. SAAL "LOAD-BEARING CAPACITY OF PERFORATED TRAPEZOIDAL SHEETING" STABILITY AND DUCTILITY OF STEEL STRUCTURES, RIO DE JANEIRO, BRAZIL, SEPTEMBER 8-10, 2010
[14] K. KATHAGE, Th. MISIEK, H. SAAL "STIFFNESS AND CRITICAL BUCKLING LOAD OF PERFORATED SHEETING" THIN-WALLED STRUCTURES 44, 2006
[15] DIN 18807-1:1987-06: TRAPEZPROFILE IM HOCHBAU; STAHLTRAPEZPROFILE; ALLGEMEINE ANFORDERUNGEN, ERMITTLUNG DER RAGFÄHIGKEITSWERTE DURCH BERECHNUNG.
[16] DIN 18807-6:1995-09: TRAPEZPROFILE IM HOCHBAU; ALUMINIUM-TRAPEZPROFILE UND IHRE VERBINDUNGEN; ERMITTLUNG DER TRAGFÄHIGKEITSWERTE DURCH BERECHNUNG